Accepted Manuscript

A novel chromone and rhodamine derivative as fluorescent probe for the detection of Zn(II) and Al(III) based on two different mechanisms

Bing-jie Pang, Chao-rui Li, Zheng-yin Yang

PII:	S1386-1425(18)30618-8
DOI:	doi:10.1016/j.saa.2018.06.076
Reference:	SAA 16235
To appear in:	*Spectrochimica Acta Part A: Molecular and Biomolecular Spectroscopy*
Received date:	7 April 2018
Revised date:	19 June 2018
Accepted date:	20 June 2018

Please cite this article as: Bing-jie Pang, Chao-rui Li, Zheng-yin Yang , A novel chromone and rhodamine derivative as fluorescent probe for the detection of Zn(II) and Al(III) based on two different mechanisms. Saa (2018), doi:10.1016/j.saa.2018.06.076

A novel chromone and rhodamine derivative as fluorescent probe for the detection of Zn(Ⅱ) and Al(Ⅲ) based on two different mechanisms

*Bing-jie Pang, Chao-rui Li, Zheng-yin Yang**

College of Chemistry and Chemical Engineering, State Key Laboratory of Applied Organic Chemistry, Lanzhou University, Lanzhou 730000, PR China

Abstract

In this study, a novel fluorescent probe, 6-hydroxychromone-3-carbaldehyde-(rhodamine B carbonyl) hydrazine (**L**), for Zn^{2+} and Al^{3+} was designed and synthesized. Initially, this probe **L** exhibited inferior fluorescence emission peak centered at 488 nm in EtOH/HEPES solution (3/1, 10.0 μM HEPES, pH 7.4) when excited at 421 nm. After the addition of Zn^{2+}, this probe **L** displayed excellent selectivity towards Zn^{2+} with obvious fluorescence color change from colorless to yellow, which might be attributed to the formation of a 1 : 1 ligand-metal complex resulting in the inhibition of photo-induced electron transfer phenomenon. Whereas, the prepared Zn^{2+} complex of **L** could be used as a ratiometric fluorescent probe to detect Al^{3+} on the basis of fluorescence resonance energy transfer mechanism. This ligand-metal complex of Zn^{2+} (**LZn**) showed high selectivity towards Al^{3+} with obvious enhancement in fluorescence emission intensity at 580 nm and remarkable decrease in fluorescence emission intensity at 488 nm, and the fluorescence color also changed from yellow to pink. Furthermore, the detection limit of the probe **L, LZn** toward Zn^{2+}, Al^{3+} were 1.25×10^{-7} M and 3.179×10^{-6} M, respectively. Additionally, the complexation properties of **L** towards Zn^{2+} and **LZn** towards Al^{3+} were studied in detail.

Keywords: Fluorescent probe; Rhodamine; Chromone; Zn^{2+}; Al^{3+}; FRET

Introduction

Zinc is considered to be the second most abundant transition metal ion in the human body and plays a crucial role in a variety of physiological and pathological processes including DNA synthesis, gene expression, enzyme regulation structure and neuronal signal transmission and so on [1-3]. Thus, an appropriate amount of Zn^{2+} is beneficial for the human health. However, excessive amount of Zn^{2+} exhibits toxicity and causes many severe diseases such as Alzheimer's disease, Parkinson's disease [4-7]. Therefore, it is worthwhile to develop new methods for the detection of Zn^{2+}.

Aluminum is the most abundant metal element in the earth's crust and aluminum compounds are extensively utilized in defense scientific researches, manufacturing, and other fields, bringing great convenience to human society [8-10]. Nevertheless, aluminum also has some adverse effects on people's life. Al^{3+} can accumulate in the human body through food chains and enrich in the body eventually, which can lead to a variety of health issues, such as impairment of memory, Alzheimer's disease, Parkinson's disease and bone softening [11-17]. Since Al^{3+} is closely related to human health, it is significantly important to develop several highly selective and convenient tools for the detection of Al^{3+}.

In recent years, fluorescent probes have been widely used for the detection of various metal ions due to their advantages like real-time detection, high selectivity and versatility [18-30]. Especially, the ratiometric fluorescent probes can avoid the effects of a series of external factors, such as intensity of the light source, scattering and

coloration of the media, and the development of them has attracted the attention of researchers [31, 32]. Meanwhile, among various mechanisms already proposed for metal ions sensing on a basis of ratiometric fluorescence response, fluorescence resonance energy transfer (**FRET**) is more advantageous than internal charge transfer (**ICT**) [33]. More importantly, to the best of our knowledge, there have been relatively few studies focused on using of ligand-metal complexes as probes to identify metal ions.

Rhodamine and its derivatives have been widely utilized for designing of fluorescent probes due to their excellent photophysical properties such as high extinction coefficient, excellent quantum yields and great photostability. It is well known that rhodamine spirolactam derivatives have no fluorescence emission and no fluorescence color. Nevertheless, when a specific metal ion is added, it triggers the ring-opening reaction of rhodamine and emits its characteristic emission peak [30, 34-36]. Due to the excellent spectroscopic and pharmacological properties, chromone derived compounds have drawn special attention in the study of fluorophores and antitumoral agents [37].

Herein, for these reasons, we have presented the design and synthesis of a new type of rhodamine and chromone derived fluorescent probe called 6-hydroxychromone-3-carbaldehyde-(rhodamine B carbonyl) hydrazine (**L**) for the differential detection of Zn^{2+} and Al^{3+}. Upon the addition of Zn^{2+}, this probe **L** showed a significant enhancement in fluorescence emission intensity at 488 nm in EtOH/HEPES solution

(3/1, 10.0 μM HEPES, pH 7.4), which might be attributed to the formation of a 1 : 1 ligand-metal complex resulting in the inhibited the photo-induced electron transfer (**PET)** process. More importantly, the ligand-metal complex **LZn** could detect Al^{3+} in a ratiometric way based on **FRET** mechanism. This complex **LZn** displayed high selectivity towards Al^{3+} in Ethanol/MeCN/HEPES solution (6/1/1, 10.0 μM HEPES, pH 7.4) with significant enhancement in fluorescence intensity emission at 580 nm while remarkable decrease in fluorescence emission intensity at 488 nm.

Experimental

Materials and instrumentation

All chemicals and reagents were obtained from commercial suppliers and used as received without further purification. ^{1}H NMR spectra were measured on the JNM-ECS 400 MHz instruments using DMSO-d_6 as a solvent and TMS as an internal standard. ESI-MS spectra were determined on a Bruker esquire 6000 spectrometer in absolute ethanol. UV–vis absorption spectra were determined on a UV-240 spectrophotometer (Shimadzu). Fluorescence emission spectra were recorded on a RF-5301 spectrophotometer (Hitachi) equipped with quartz cuvettes of 1 cm path length. The melting points were recorded on a Beijing XT4-100 microscopic melting point apparatus without correction.

Synthesis

6-Hydroxyl-3-formyl chromone (compound **1**) [38] and rhodamine B hydrazide (compound **2**) [39] were obtained according to the reported procedures. Synthesis of

fluorescent probe **L** was based on the following method (Scheme 1): an ethanol solution (25 mL) of rhodamine B hydrazide (0.457 g, 1 mmol) was added to another solution of 6-Hydroxyl-3-formyl chromone (0.190 g, 1 mmol) in ethanol (25 mL). Then the mixture was refluxed for 12 h under stirring, during which time some light pink precipitant appeared. After the reaction was completed, the reaction mixture was cooled to room temperature. Subsequently, the precipitant was filtered under reduced pressure, washed 3 times with ethanol (10 mL). Then the precipitant was dried in vacuo and pink solid was obtained. Yield: 72.0%. M.P.: 264-266 ℃. ^{1}H NMR (DMSO-d_6, 400 MHz): δ 10.12 (s, 1H, H^{13}), 8.70 (s, 1H, H^8), 8.33 (s, 1H, H^{12}), 7.91 (d, 1H, J = 6.8 Hz, H^7), 7.61 (td, 1H, J = 7.2 Hz, J = 1.2 Hz, H^5), 7.55 (td, 1H, J = 7.6 Hz, J = 0.8 Hz, H^6), 7.51 (d, 1H, J = 8.8 Hz, H^9), 7.26 (d, 1H, J = 2.8 Hz, H^{11}), 7.21 (dd, 1H, J = 8.8 Hz, J = 2.8 Hz, H^{10}), 7.07 (d, 1H, J = 7.6 Hz, H^4), 6.45 (d, 2H, J = 2.4 Hz, H^1), 6.41 (d, 2H, J = 8.8 Hz, H^3), 6.33 (dd, 2H, J = 8.8 Hz, J = 2.6 Hz, H^2), 3.31 (q, 8H, J = 14 Hz, J = 6.8 Hz, H^{14}), 1.07 (t, 12H, J = 6.8 Hz, H^{15}), (Fig. S1). MS (ESI): m/z 629.39 $[M + H]^+$, (Fig. S2).

Analysis

Stock solutions of various metal ions (5 mM) were prepared in water from $Al(NO_3)_3$, $AgNO_3$, $BaCl_2$, $Ca(NO_3)_2$, $Cd(NO_3)_2$, $CrCl_3$, $CoCl_2$, $Cu(NO_3)_2$, $FeCl_3$, $HgCl_2$, KNO_3, $LiNO_3$, $Mn(NO_3)_2$, $NaNO_3$, $Ni(NO_3)_2$, $PB(NO_3)_2$ and $Zn(NO_3)_2$. Stock solution of fluorescent probe **L** (5 mM) was prepared in DMSO. Test solutions were prepared by placing 20 μL of the probe **L** and **LZn** stock solution into cuvettes, adding an appropriate aliquot of various metal ions solutions, and diluting the solution to 2 mL

with EtOH/HEPES solution (3/1, 10.0 μM HEPES, pH 7.4) and EtOH/MeCN/HEPES solution (6/1/1, 10.0 μM HEPES, pH 7.4) respectively. After mixing fluorescent probe **L** and **LZn** with metal ions for 10 min, the UV-vis absorption spectra and fluorescence emission spectra were recorded at room temperature. For all fluorescence measurements, the excitation and emission slit widths were both set at 5 nm.

Results and discussion

*Sensing behavior of **L** towards Zn^{2+}*

In order to study the binding ability between **L** and Zn^{2+}, the UV-vis absorption spectra of **L** in the absence and presence of various metal ions were recorded in EtOH/HEPES solution (3/1, 10.0 μM HEPES, pH 7.4), and the results were illustrated in Fig. 1. Upon addition of Zn^{2+} (1.0 *equiv.*), the absorption bands centered at 421 nm and 450 nm assigned to the chromone moiety enhanced and their absorbance reached a maximum in the presence of 1.0 *equiv.* Zn^{2+} (Fig. 1a), while almost no significant enhancement in these two absorption bands were observed in the presence of other metal ions (1.0 *equiv.*) (Fig. 1b). In addition, in the presence of Zn^{2+}, the probe **L** did not exhibit an absorption band from 485 nm to 600 nm, which indicated that rhodamine moiety of **L** was in the ring-closed isomeric form. Nevertheless, the addition of Al^{3+}, Fe^{3+} and Cr^{3+} (1.0 *equiv.*) to **L** solution led to the appearance of two new absorption bands centered at 520 nm and 560 nm, which was attributed to the ring opening reaction of the rhodamine core. In the presence of Cu^{2+} and Co^{2+}, the probe **L** only showed one absorption band centered at 560 nm, which might be attributed to the color change of

L solution**.** These results suggested that **L** could form a stable complex with Zn^{2+}.

The fluorescence emission spectra of **L** in the absence and presence of various metal ions demonstrated a similar behavior to UV-vis absorption spectra. As shown in Fig. 2, when it was excited at 421 nm, the free probe **L** solution displayed a weak fluorescence emission band and was colorless. However, after adding a variety of metal ions to **L** solution, this probe **L** did not give any visible responses to these metal ions except for Zn^{2+} at 488 nm. With the increasing concentration of Zn^{2+}, the fluorescence emission intensity of **L** at 488 nm enhanced gradually, and reached a maximum in the presence of 1.0 *equiv.* of Zn^{2+}. The quantum yield of **L** increased from 0.02 in the absence of Zn^{2+} to 0.17 for the **L**-Zn^{2+} complex. Simultaneously, the color of probe **L** solution changed from colorless to light yellow（Fig. 4）. Additionally, almost no enhancement in the fluorescence emission intensity of **L**-Zn^{2+} was observed at 580 nm, but the addition of Al^{3+}, Fe^{3+} and Cr^{3+} (1.0 *equiv.*) to probe **L** solution engendered significant fluorescence enhancement at 580 nm and the color of **L** solution changes from colorless to pink were observed, which showed that the presence of Zn^{2+} did not interfere with the spirolactam form of the rhodamine core, and the rhodamine core was in the ring-opened isomeric form in the presence of Al^{3+}, Fe^{3+} and Cr^{3+}. Therefore, the mechanism for the investigation of Zn^{2+} by probe **L** should be attributed to the interaction of the chromone moiety with Zn^{2+} which inhibited the **PET** process rather than the ring opening reaction of the rhodamine spirolactam.

In addition, we performed competition experiments by adding Zn^{2+} (1.0 *equiv.*) to

probe **L** solution in the presence of other completing metal ions (1.0 *equiv.*) to explore the property of this probe **L**. As shown in Fig. 3, we could find that the other metal ions except for Cu^{2+}, Cr^{3+}, Fe^{3+}, Al^{3+} and Ni^{2+} did not cause any significant interferences with the detection of Zn^{2+}. The fluorescence emission at 488 nm of **L** was almost quenched in the presence of Cu^{2+}, Cr^{3+} and Fe^{3+}, which might be related to the magnetic properties of these three metal ions. The response of probe **L** to Zn^{2+} in the presence of Ni^{2+} and Al^{3+} were relatively low but could be clearly detectable. Therefore, **L** was shown to be a promising fluorescent probe for the detection of Zn^{2+} in the presence of most other metal ions.

Subsequently, to investigate the binding stoichiometry between this probe **L** and Zn^{2+}, the Job's plot experiment was carried out. As depicted in Fig. 5, the maximum point appeared at a mole fraction of 0.5, which proved that probe **L** formed a 1 : 1 ligand-metal complex with Zn^{2+}. In addition, the binding stoichiometry between probe **L** and Zn^{2+} was further confirmed by the appearance of a peak at m/z 754.1179 that was assigned to $[\mathbf{L} + Zn^{2+} + NO_3^-]^+$ in the ESI-MS spectra (Fig. S2). Furthermore, the fluorescence intensity of probe **L** at 488 nm afforded a good linear relationship with the concentration of Zn^{2+} (5.0-50.0 mM). According to the fluorescence titration experiments of **L** towards increasing amounts of Zn^{2+}, the detection limit of probe **L** for sensing Zn^{2+} was calculated to be 1.25×10^{-7} M ($R^2 = 0.968$) based on an equation of $LOD = 3\sigma/k$ [40, 41] (Fig. S3) and the association constant K_a between probe **L** and Zn^{2+} was found to be 3.850×10^4 M^{-1} ($R^2 = 0.996$) with a good linear relationship by

the Benesi-Hildebrand method (Fig. S4) [42].

^{1}H NMR titration experiments were recorded in DMSO-d_6 solution to further explore the combination mode of **L** with Zn^{2+}. As illustrated in Fig. 6, upon addition of Zn^{2+} to **L** solution, the proton signals of H^7 and H^{12} were shifted upfield ($\Delta\delta$= 0.0195 ppm and 0.105 ppm, respectively), and the proton signals of H^8 and H^{11} were shifted downfield ($\Delta\delta$= 0.182 ppm and 0.0265 ppm, respectively). These results clearly suggested that the nitrogen atom of -CH=N- group, the oxygen atom of the carbonyl group from chromone unit and the oxygen atom of the carbonyl group from rhodamine moiety in **L** participated in the coordination with Zn^{2+}. Therefore, we proposed the binding mode of the complex **LZn** as shown in Scheme 2.

*Sensing behavior of **LZn** towards Al^{3+}*

As described above, in the presence of Al^{3+}, Cr^{3+} and Fe^{3+}, this probe **L** exhibited a characteristic fluorescence emission band of rhodamine centered at 580 nm and the color of probe **L** solution changed from colorless to pink. Nevertheless, the addition of Zn^{2+} (1.0 *equiv.*) to probe **L** solution engendered significant enhancement in fluorescence emission intensity at 488 nm which belonged to the chromone moiety and we could advert that almost no emission bands ranging from 500 nm to 600 nm emerged. According to previously reported literatures, 3-carbaldehyde chromone could coordinate with Zn^{2+} and emit fluorescence, the rhodamine core was in the ring-closed isomeric form and the spirolactam form of rhodamine was not disturbed in the presence of Zn^{2+}. However, when Al^{3+} or Fe^{3+} was present, it easily led to the ring-opening

reaction of rhodamine and displayed a characteristic fluorescent emission of rhodamine core [32, 43-46]. Therefore, the spirolactam structure of the rhodamine unit in such ligand-metal complex might be further transferred into ring-opened isomeric form, giving a characteristic fluorescent emission that belonged to rhodamine in the presence of Al^{3+}, Cr^{3+} and Fe^{3+}. Thus, the ligand-metal complex **LZn** might be used as a probe to identify other metal ions, such as Al^{3+}. To verify this conjecture, we prepared this ligand-metal complex **LZn** by mixed **L** (50 μM) with 1.0 *equiv.* of Zn^{2+} in Ethanol/MeCN/HEPES solution (6/1/1, 10.0 μM HEPES, pH 7.4) and carried out the further experiments.

The selectivity of **LZn** towards Al^{3+} was investigated in Ethanol/MeCN/HEPES solution (6/1/1, 10.0 μM HEPES, pH 7.4). As shown in Fig. 8, this ligand-metal complex **LZn** showed yellow fluorescence emission at 488 nm corresponding to chromone moiety when it was excited at 467 nm. However, the addition of Al^{3+} to **LZn** solution immediately triggered a much more significant red-shift of 92 nm in fluorescence emission spectra and a new emission peak centered at 580 nm emerged, which might be ascribed to a **FRET** process from excited 6-Hydroxyl-3-formyl chromone moiety to ring-opened rhodamine unit [45, 46]. Nevertheless, upon the addition of other various metal ions such as Ag^{+}, Ba^{2+}, Ca^{2+}, Co^{2+}, Cr^{3+}, Cu^{2+}, Fe^{3+}, Hg^{2+}, K^{+}, Li^{+}, Mg^{2+}, Mn^{2+}, Na^{+}, Ni^{2+} and Pb^{2+} to the solution of **LZn,** almost no observable responses at 580 nm were obtained except for Cr^{3+} and Fe^{3+}, only Cr^{3+} and Fe^{3+} caused a relatively weak emission band centered at 580 nm, it did not remarkably

interfere with the detection of Al^{3+} by **LZn**. Additionally, the presence of Cu^{2+} caused the fluorescence emission of **LZn** at 488 nm to almost completely quenched, which was due to the magnetic property of Cu^{2+}. These results strongly supported the conclusion that **LZn** could be utilized as a selective ratiometric fluorescent probe based on the **FRET** mechanism for sensing Al^{3+}.

The interaction between **LZn** and Al^{3+} was then investigated by measuring the change in UV-vis absorption spectra of **LZn** (50 μM) with addition of Al^{3+} (1.0 *equiv.*). As shown in Fig. 7, upon the addition of Al^{3+} (1.0 *equiv.*) into **LZn** solution, the absorption bands centered at 405 nm, 421 nm and 450 nm obviously decreased with concomitant formation of two new absorption bands centered at 520 nm and 560 nm, and the color of the **LZn** solution changed from yellow to pink, which further suggested that the rhodamine core of **LZn** was in the ring-closed isomeric form and the spirolactam form of rhodamine could be transformed into the ring-open isomeric form in the presence of Al^{3+}. Furthermore, the fluorescence titration experiments of **LZn** were also recorded upon excitation at 467 nm. As shown in Fig. 8, the addition of Al^{3+} (1.0 *equiv.*) to **LZn** solution aroused a significant increase in fluorescence emission intensity at 580 nm with a decrease in the emission peak of **LZn** at 488 nm, and the quantum yield of **LZn** increased to 0.44. the ratio of fluorescence emission intensity at 580 nm and 488 nm (F_{580}/F_{488}) changed about 331.4 times (from 0.137 to 45.4) and reached a maximum in the presence of 1.0 *equiv.* of Al^{3+}, which was consistent with the results from UV-vis titration experiments, suggesting that the recognition molar ratio

between **LZn** and Al^{3+} might be 1:1.

One of the significant properties of a good probe is its high selectivity towards the target metal ion exceeding other competing metal ions. Therefore, the competition experiments of **LZn** were carried out in Ethanol/MeCN/HEPES solution (6/1/1, 10.0 μM HEPES, pH 7.4). For this purpose, competitive ions were firstly added to the **LZn** solution, and then Al^{3+} (1.0 *equiv.*) was added after 10 min. The results shown in Fig. 10 confirmed that most of other competitive metal ions showed relatively low interference with the detection of Al^{3+}, only Cu^{2+} had posed an effect on the fluorescence response of **LZn** to Al^{3+} that was due to the magnetic property of Cu^{2+}. Moreover, Cr^{3+} decreased the fluorescence emission intensity ratio (F_{580}/F_{488}) of **LZn** in the presence of Al^{3+} to a certain degree but the effect was negligible. Therefore, **LZn** was shown to be a promising ratiometric fluorescent probe for sensing Al^{3+} in the presence of most competing metal ions.

On a basis of fluorescence titration experiments, relative fluorescence intensity ratio (F_{580}/F_{488}, λ_{ex} = 467 nm) afforded a good linear relationship versus the concentration of Al^{3+} (10.0 – 50.0 μM). The detection limit of **LZn** for sensing Al^{3+} was also calculated according to the equation of $LOD = 3\sigma/k$, and the result was found to be 3.179×10^{-6} M (R^2 = 0.983) (Fig. S6). Furthermore, the association constant K_a between **LZn** and Al^{3+} was calculated to be 1.611×10^4 M^{-1} (R^2 = 0.997) with a good linear relationship by the Benesi-Hildebrand method (Fig. S7).

The binding stoichiometry between **LZn** and Al^{3+} was confirmed by the ESI-MS

spectra in ethanol. As can be seen from Fig. S8, the peak at m/z 779.1659 corresponding to [**LZn** - Zn^{2+} + Al^{3+} + $2NO_3^-$]$^+$ and the peak at m/z 762.2143 corresponding to [**LZn** - Zn^{2+} + Al^{3+} + NO_3^- + EtOH – H^+]$^+$ were clearly observed in the ESI-MS spectra, which indicated that **LZn** reacted with Al^{3+} in a 1 : 1 ratio and Zn^{2+} in **LZn** was replaced by Al^{3+} during this reaction process. In addition, ^{1}H NMR studies provided additional evidence of the interaction between **LZn** and Al^{3+}. For this purpose, ^{1}H NMR spectra of **LZn** were recorded in DMSO-d_6 solution upon addition of Al^{3+}. As shown in Fig. 11, when Al^{3+} was added to **LZn** in DMSO-d_6 solution, the proton signal of imino group (-NH-) emerged at 9.18ppm. Furthermore, the peaks of H^7 and H^{12} were shifted downfield ($\Delta\delta$ = 0.0225 ppm and 0.100 ppm, respectively), and the peaks of H^8 and H^{11} were shifted upfield ($\Delta\delta$ = 0.207 ppm and 0.0265 ppm, respectively). These results suggested that the imino N, rhodamine carbonyl O, and chromone carbonyl O atoms participated in the coordination with Al^{3+}. More importantly, the appearance of the proton signal for imino group (-NH-) clearly proved that the rhodamine core in **LZn** was in the ring-opened isomeric form in the presence of Al^{3+}. On a basis of the results above, the proposed binding mode of **LZn** with Al^{3+} was deduced and illustrated in Scheme 2.

*Application of **L** as a solid state probe*

According to the previous experiments, this probe **L** solution emitted yellow fluorescence after adding Zn^{2+}. Inspired by this, we tested the practical applicability of utilizing **L** as a solid state probe for the detection of Zn^{2+}. For this purpose, **L** was

adsorbed on the filter papers by immersing filter papers in the EtOH/HEPES solution (3/1, 10.0 μM HEPES, pH 7.4) of **L** (1 mM) and then drying them in the air for 12 hours. Subsequently, the solutions of various metal ions (1 mM) at the same concentration were dropped in these test strips, and their photographs under a 365 nm UV lamp were shown in Fig. 12. The color of the coated test paper changed from black to yellow with the addition of Zn^{2+} under illumination using a 365 nm UV lamp, indicating that this probe **L** could also recognize Zn^{2+} in the solid state. Nevertheless, only Al^{3+} caused a color changed of coated test paper from black to light pink under a 365 nm UV lamp but it could be clearly distinguished from that in the presence of Zn^{2+}. Furthermore, the introduction of other competitive metal ions did not lead to any color changes of coated test paper. As a result, this probe **L** exhibited excellent fluorescence sensing performance even in the solid state and could be applied for the detection of Zn^{2+} in practical samples [47].

Conclusion

In conclusion, a novel chromone and rhodamine derivative as fluorescent probe for the detection of Zn^{2+} and Al^{3+} based on two different mechanisms was reported. This probe **L** exhibited high selectivity towards Zn^{2+} (excitation at 421 nm and emission at 488 nm) over other metal ions and high sensitivity for Zn^{2+} with the detection limit reaching 10^{-7} level in the EtOH/HEPES solution (3/1, 10.0 μM HEPES, pH 7.4). The selective recognition of **L** towards Zn^{2+} should be attributed to the interaction of the chromone moiety with Zn^{2+} which inhibited the **PET** process. Furthermore, we found

that the ligand-metal complex **LZn** could be utilized as a ratiometric fluorescent probe to selectively sense Al^{3+} (excitation at 467 nm and emission at 580 nm) on a basis of the **FRET** mechanism. The addition of Al^{3+} to **LZn** solution triggered a much more remarkable red-shift of 92 nm in fluorescence emission spectra and a new emission peak centered at 580 nm emerged. To the best of our knowledge, the Zn^{2+} complex of chromone derivatives which could be used as new **FRET** fluorescent probes are relatively rare (Table. 1.). More importantly, this probe **L** displayed an excellent fluorescence sensing performance even in the solid state. This strategy might provide a general way for designing new **FRET** probes for detecting other environmentally and biologically relevant species.

Acknowledgments

This work is supported by the National Natural Science Foundation of China (21761019)

Reference

[1] X. Xie, T.G. Smart, Nature 349 (1991) 521.

[2] B.L. Vallee, K.H. Falchuk, Physiol. Rev. 73 (1993) 79–118.

[3] Q. Ai, Biometals 14 (2001) 315–330.

[4] A.I. Bush, Trends Neurosci. 26 (2003) 207-214.

[5] R. Sladek, G. Rocheleau, J. Rung, C. Dina, L. Shen, D. Serre, et al., Nature 445 (2007) 881-885.

[6] E. Ho, J. Nutr. Biochem. 15 (2004) 572-578.

[7] P. Jiang, Z. Guo, Coordin. Chem. Rev. 248 (2004) 205-229.

[8] C.C. Jayme, I.R. Calori, A.C. Tedesco, Spectrochim. Acta, Part A 153 (2016) 178-183.

[9] M.A. Nunes, A.S.G. Costa, J.C.M. Barreira, A.F. Vinha, R.C. Alves, A. Rocha, et al., LWT - Food Sci. Technol. 65 (2016) 70-78.

[10]R.A. Yokel, R.L. Florence, Toxicol. Lett. 227 (2006) 86-93.

[11]D.P. Perl, D.C. Gajdusek, R.M. Garruto, R.T. Yanagihara, C.J. Gibbs, Science 217 (1982) 1053–1055.

[12]J.L. Smith, S. Xiong, W.R. Markesbery, M.A. Lovell, Neuroscience 140 (2006) 879-888.

[13]O. Tavakoli, H. Yoshida, Environ. Sci. Technol. 39 (2005) 2357–2363.

[14]D.P. Perl, A.R. Brody, Science 208 (1980) 297–299.

[15]G.D. Fasman, Coord. Chem. Rev. 149 (1996) 125–165.

[16]P.D. Darbre, F. Mannello, C. Exley, J. Inorg. Biochem. 128 (2013) 257-261.

[17]S.C. Bondy, Neurotoxicology 52 (2016) 222-229.

[18]J. Afshani, A. Badiei, N. Lashgari, G. Mohammadi Ziarani, RSC Adv. 6 (2016) 5957-5964.

[19]M.J. Chang, M.H. Lee, Dyes Pigments 149 (2018) 915-920.

[20]Y. Dong, T. Liu, X. Wan, H. Pei, L. Wu, Y. Yao, Sensor. Actuat. B-Chem. 241 (2017) 1139-1144.

[21]D. Kong, F. Yan, Y. Luo, Q. Ye, S. Zhou, L. Chen, Anal. Chim. Acta 953 (2017) 63-70.

[22]N. Lashgari, A. Badiei, G. Mohammadi Ziarani, J. Fluoresc. 26 (2016) 1885-1894.

[23]Y.S. García-Gutiérrez, C.A. Huerta-Aguilar, P. Thangarasu, J.M. Vázquez-Ramos, Sensor. Actuat. B-Chem. 248 (2017) 447-459.

[24]F.U. Rahman, A. Ali, S.K. Khalil, R. Guo, P. Zhang, H. Wang, et al., Talanta 164 (2017) 307-313.

[25]S. Suganya, J.W. Namgoong, A.K. Mutyala, S. Velmathi, J.P. Kim, J.S. Park, J. Photoch. Photobio. A 344 (2017) 36-41.

[26]L. Tang, S. Ding, K. Zhong, S. Hou, Y. Bian, X. Yan, Spectrochim. Acta, Part A 174 (2017) 70-74.

[27]L. Wang, W. Li, W. Zhi, Y. Huang, J. Han, Y. Wang, et al., Sensor. Actuat. B-Chem. 260 (2018) 243-254.

[28]Y. Xu, S. Mao, H. Peng, F. Wang, H. Zhang, S.O. Aderinto, etal., J. Lumin. 192 (2017) 56-63.

[29]S.A. Yoon, J. Lee, M.H. Lee, Sensor. Actuat. B-Chem. 258 (2018) 50-55.

[30]Y. Chen, Y. Mi, Q. Xie, J. Xiang, H. Fan, X. Luo, et al., Anal. Methods-UK. 5 (2013) 4818.

[31]Y. Ge, X. Xing, A. Liu, R. Ji, S. Shen, X. Cao, Dyes Pigments. 146 (2017) 136-142.

[32]T. Liu, X. Wan, Y. Yao, Sensor. Actuat. B-Chem. 254 (2018) 1094-1100.

[33]L.J. Zhang, Z.Y. Wang, J.T. Liu, J.Y. Miao, B.X. Zhao, Sensor. Actuat. B-Chem.

253 (2017) 19-26.

[34]H. Kim, S.H. Kim, D.H. Lee, Y.A. Son, Supramol. Chem. 25 (2013) 87-91.

[35]H.N. Kim, M.H. Lee, H.J. Kim, J.S. Kim, J. Yoon, Chem. Soc. Rev. 37 (2008) 1465-1472.

[36]C. Wang, K.M. Wong, Inorg. Chem. 52 (2013) 13432-13441.

[37]R.T. Cummings, J.P. Dizio, G.A. Krafft, Tetrahedron Lett. 29 (1988) 69-72.

[38]B.D. Wang, Z.Y. Yang, D.W. Zhang, Y. Wang, Spectrochim. Acta, Part A 63 (2006) 213-219.

[39]V. Dujols, F. Ford, A.W. Czarnik, J. Am. Chem. Soc. 119 (1997) 7386–7387.

[40]L. Mei, Y. Xiang, N. Li, A. Tong, Talanta 72 (2007) 1717-1722.

[41]H.M. Park, B.N. Oh, J.H. Kim, W. Qiong, I.H. Hwang, K.D. Tetrahedron Lett. 52 (2011) 5581-5584.

[42]H.A. Benesi, J.H Hildebrand, J. Am. Chem. Soc. 71 (1949) 2703-2707

[43]G. Xie, Y. Shi, F. Hou, H. Liu, L. Huang, P. Xi, et al., Eur. J. Inorg. Chem. 2012 (2012) 327-332.

[44]X. Zhou, W. Yan, T. Zhao, Z. Tian, X. Wu, Tetrahedron 69 (2013) 9535-9539.

[45]S. Erdemir, M. Yuksekogul, S. Karakurt, O. Kocyigit, Sensor. Actuat. B-Chem. 241 (2017) 230-238.

[46]C.Y. Li, Y. Zhou, Y.F. Li, C.X. Zou, X.F. Kong, Sensor. Actuat. B-Chem. 186 (2013) 360-366.

[47]G. Dhaka, N. Kaur, J. Singh, Inorg. Chim. Acta 464 (2017) 18-22.

Figure captions

Scheme 1. Synthetic route of **L**.

Fig. 1. (a) UV-vis absorption spectra of **L** (50.0 μM) in EtOH/HEPES solution (3/1, 10.0 μM HEPES, pH 7.4) after addition of Zn^{2+} (0, 0.1, 0.2, 0.3, 0.4, 0.5, 0.6, 0.7, 0.8, 0.9, 1.0 *equiv.*). Insert: the color changes of **L** solution (50.0 μM) in the absence and presence of Zn^{2+} (1.0 *equiv.*); (b) Absorption changes of **L** upon addition of different metal ions (50.0 μM).

Fig. 2. Fluorescence emission spectra of **L** (50 μM) upon the addition of various metal ions (1.0 *equiv.*) of Ag^{+}, Al^{3+}, Ba^{2+}, Ca^{2+}, Co^{2+}, Cr^{3+}, Cu^{2+}, Fe^{3+}, Hg^{2+}, K^{+}, Li^{+}, Mg^{2+}, Mn^{2+}, Na^{+}, Ni^{2+}, Pb^{2+} and Zn^{2+} in EtOH/HEPES solution (3/1, 10.0 μM HEPES, pH 7.4) (λ_{ex} = 421 nm, Slit widths: 5 nm/5 nm). Inset: color of **L** (left) and **L** + Zn^{2+} (right) system under UV lamp.

Fig. 3. Fluorescence emission intensity at 488 nm of **L** and its complexation with Zn^{2+} in the presence of other various metal ions (Ag^{+}, Al^{3+}, Ba^{2+}, Ca^{2+}, Co^{2+}, Cr^{3+}, Cu^{2+}, Fe^{3+}, Hg^{2+}, K^{+}, Li^{+}, Mg^{2+}, Mn^{2+}, Na^{+}, Ni^{2+} and Pb^{2+}) in EtOH/HEPES solution (3/1, 10.0 μM HEPES, pH 7.4). Black bar: **L** (50.0 μM) in the presence of 1.0 *equiv.* of various metal ions. Red bar: **L** (50.0 μM) with 1.0 *equiv.* of Zn^{2+} in the presence of 1.0 *equiv.* of other various metal ions (λ_{ex} = 421 nm).

Fig. 4. Fluorescence emission spectra of **L** (50 μM) in EtOH/HEPES solution (3/1, 10.0 μM HEPES, pH 7.4) upon gradual addition of Zn^{2+} (0-1.2 *equiv.*) (λ_{ex} = 421 nm, slit

widths: 5 nm/5 nm).

Fig. 5. Job's plot for determining the stoichiometry between probe **L** and Zn^{2+} in EtOH/HEPES solution (3/1, 10.0 μM HEPES, pH 7.4). $X_{Zn} = [Zn^{2+}]/([Zn^{2+}] + [\mathbf{L}])$, the total concentration of **L** and Zn^{2+} was 50 μM (λ_{ex} = 421 nm, slit widths: 5 nm/5 nm).

Fig. 6. ^{1}H NMR (DMSO-d_6, 400 MHz) spectra of **L** only and **L** with 1 *equiv.* of Zn^{2+}.

Fig. 7. UV-vis absorption spectra of **LZn** (50.0 μM) in EtOH/MeCN/HEPES solution (6/1/1, 10.0 μM HEPES, pH 7.4) after addition of Al^{3+} (0, 0.1, 0.2, 0.3, 0.4, 0.5, 0.6, 0.7, 0.8, 0.9, 1.0 *equiv.*). Insert: the color changes of **LZn** solution (50.0 μM) in the absence and presence of Al^{3+} (1.0 *equiv.*).

Fig. 8. (a) Fluorescence emission spectra of **LZn** (50 μM) in EtOH/MeCN/HEPES solution (6/1/1, 10.0 μM HEPES, pH 7.4) upon gradual addition of Al^{3+} (0-1.0 *equiv.*) (λ_{ex} = 467 nm, slit widths: 5 nm/5 nm). Inset: color of **LZn** (left) and **LZn** + Al^{3+} (right) system under UV lamp; (b) Plot of relative fluorescence intensity ratio (F_{580}/F_{488}, λ_{ex} = 467 nm) as a function of $[Al^{3+}]$.

Fig. 9. (a) Fluorescence emission spectra of **LZn** (50 μM) upon the addition of various metal ions (Ag^+, Ba^{2+}, Ca^{2+}, Co^{2+}, Cr^{3+}, Cu^{2+}, Fe^{3+}, Hg^+, K^+, Li^+, Mg^{2+}, Mn^{2+}, Na^+, Ni^+, Pb^{2+} and Al^{3+}) (1.0 *equiv.*) in EtOH/MeCN/HEPES solution (6/1/1, 10.0 μM HEPES, pH 7.4); (b) Relative fluorescence intensity ratio (F_{580}/F_{488}, λ_{ex} = 467 nm) of **LZn** (50 μM) in the absence and presence of various metal ions in EtOH/MeCN/HEPES solution (6/1/1, 10.0 μM HEPES, pH 7.4) (λ_{ex} = 467 nm, slit widths: 5 nm/5 nm).

Fig. 10. The ratio of fluorescence emission intensity at 580 nm and 488 nm (F_{580}/F_{488})

of **LZn** and its complexation with Al^{3+} in the presence of other various metal ions (Ag^{+}, Ba^{2+}, Ca^{2+}, Co^{2+}, Cr^{3+}, Cu^{2+}, Fe^{3+}, Hg^{+}, K^{+}, Li^{+}, Mg^{2+}, Mn^{2+}, Na^{+}, Ni^{+} and Pb^{2+}) in EtOH/MeCN/HEPES solution (6/1/1, 10.0 μM HEPES, pH 7.4). Black bar: **LZn** (50.0 μM) in the presence of 1.0 *equiv.* of various metal ions. Red bar: **LZn** (50.0 μM) with 1.0 *equiv.* of Al^{3+} in the presence of 1.0 *equiv.* of other various metal ions (λ_{ex} = 467 nm, slit widths: 5 nm/5 nm).

Fig. 11. ^{1}H NMR (DMSO-d_6, 400 MHz) spectra of **L** with 1 *equiv.* of Zn^{2+} (**LZn**); **LZn** with 1 *equiv.* of Al^{3+}.

Fig. 12. The photographs of coated test papers after addition of different metal ions under illumination using a 365 nm UV lamp.

Table 1. Comparison of different properties of **L** and **LZn** with recently reported probes based on rhodamine derivatives.

Scheme 2. Proposed binding mechanism of **L** with Zn^{2+} and **LZn** with Al^{3+}.

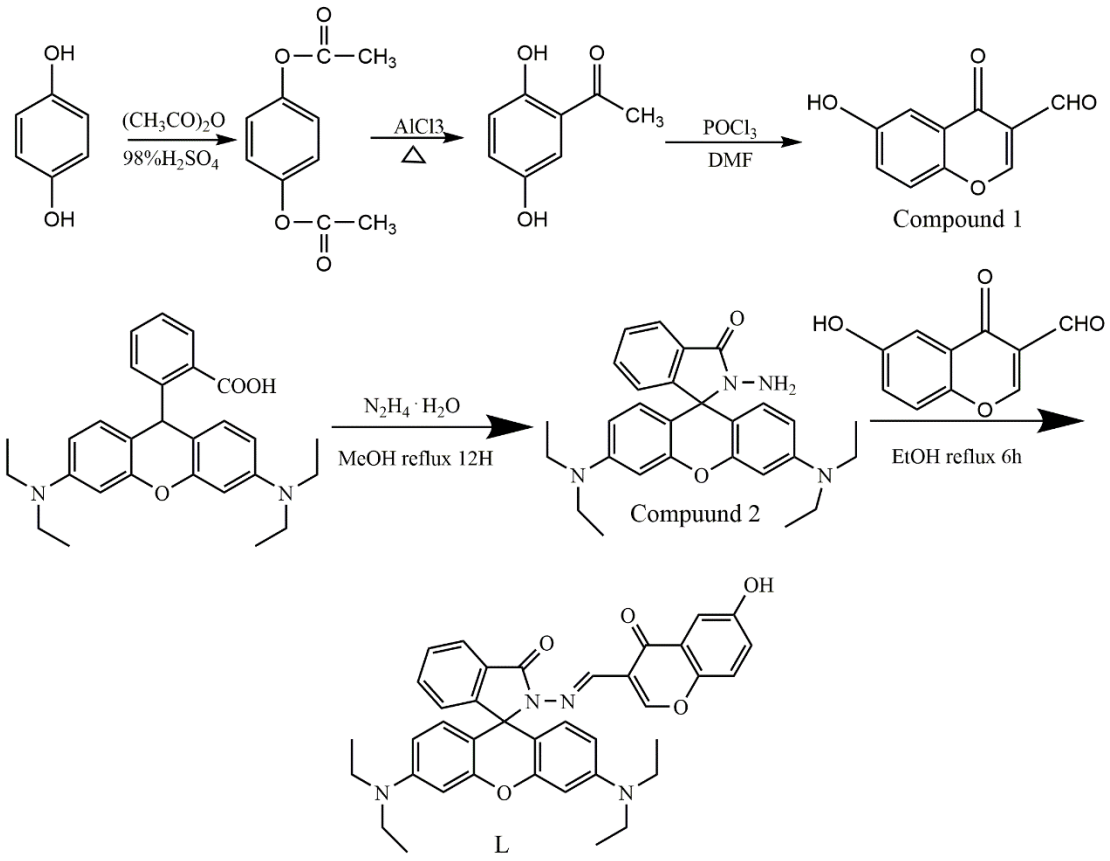

Scheme 1. Synthetic route of **L**.

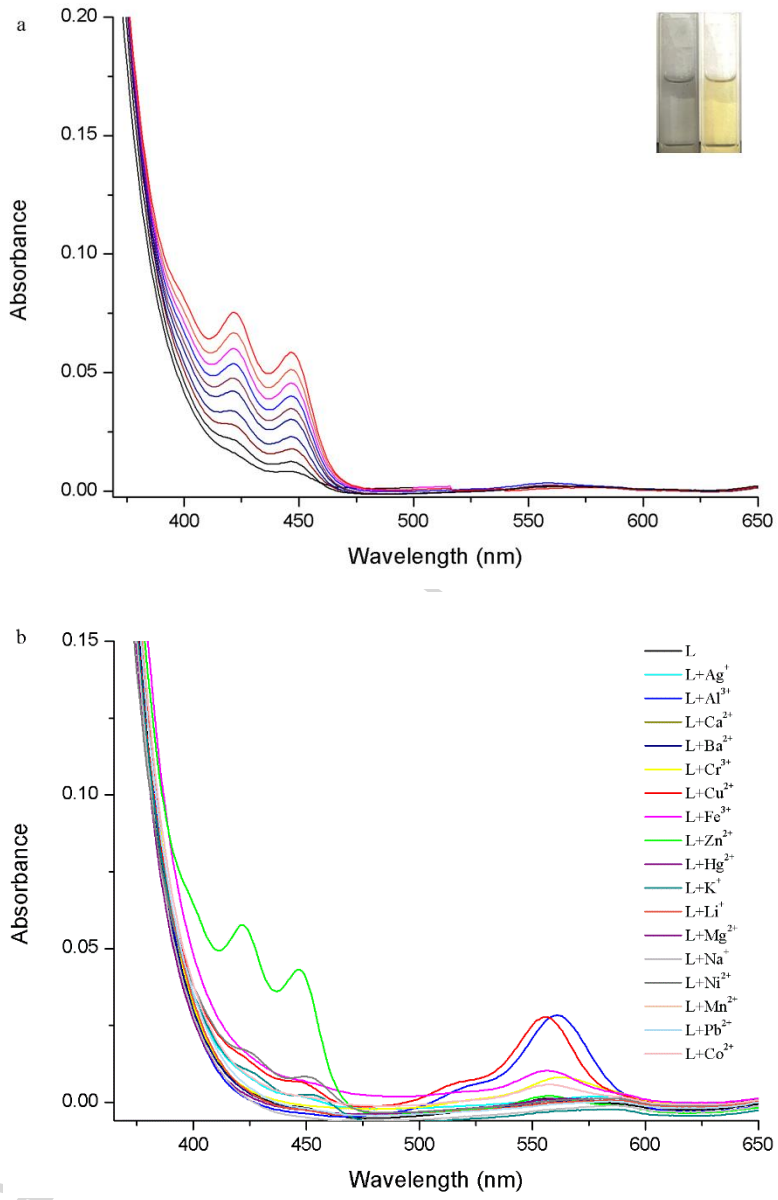

Fig. 1. (a) UV-vis absorption spectra of **L** (50.0 μM) in EtOH/HEPES solution (3/1, 10.0 μM HEPES, pH 7.4) after addition of Zn^{2+} (0, 0.1, 0.2, 0.3, 0.4, 0.5, 0.6, 0.7, 0.8, 0.9, 1.0 *equiv.*). Insert: the color changes of **L** solution (50.0 μM) in the absence and presence of Zn^{2+} (1.0 *equiv.*); (b) Absorption changes of **L** upon addition of different metal ions (50.0 μM).

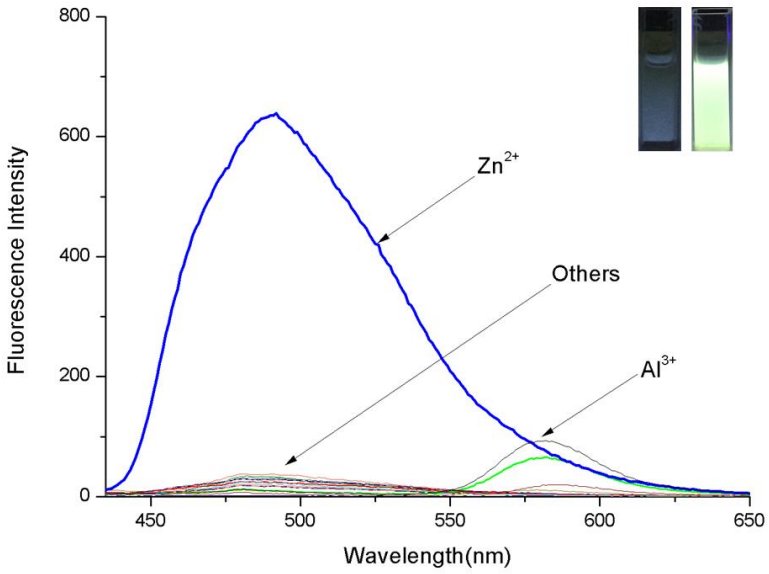

Fig. 2. Fluorescence emission spectra of **L** (50 μM) upon the addition of various metal ions (1.0 *equiv.*) of Ag^{+}, Al^{3+}, Ba^{2+}, Ca^{2+}, Co^{2+}, Cr^{3+}, Cu^{2+}, Fe^{3+}, Hg^{2+}, K^{+}, Li^{+}, Mg^{2+}, Mn^{2+}, Na^{+}, Ni^{2+}, Pb^{2+} and Zn^{2+} in EtOH/HEPES solution (3/1, 10.0 μM HEPES, pH 7.4) (λ_{ex} = 421 nm, Slit widths: 5 nm/5 nm). Inset: color of **L** (left) and **L** + Zn^{2+} (right) system under UV lamp.

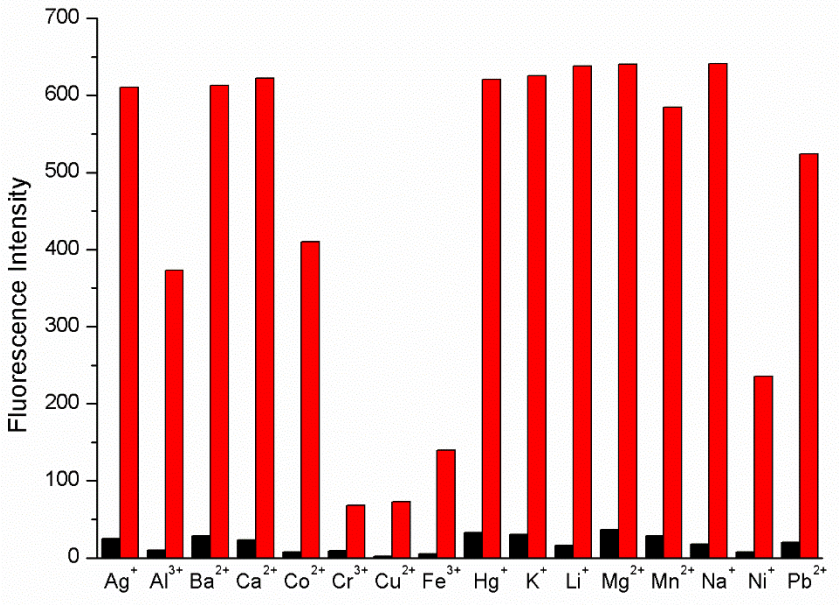

Fig. 3. Fluorescence emission intensity at 488 nm of **L** and its complexation with Zn^{2+} in the presence of other various metal ions (Ag^{+}, Al^{3+}, Ba^{2+}, Ca^{2+}, Co^{2+}, Cr^{3+}, Cu^{2+}, Fe^{3+}, Hg^{2+}, K^{+}, Li^{+}, Mg^{2+}, Mn^{2+}, Na^{+}, Ni^{2+} and Pb^{2+}) in EtOH/HEPES solution (3/1, 10.0 μM HEPES, pH 7.4). Black bar: **L** (50.0 μM) in the presence of 1.0 *equiv.* of various metal ions. Red bar: **L** (50.0 μM) with 1.0 *equiv.* of Zn^{2+} in the presence of 1.0 *equiv.* of other various metal ions (λ_{ex} = 421 nm).

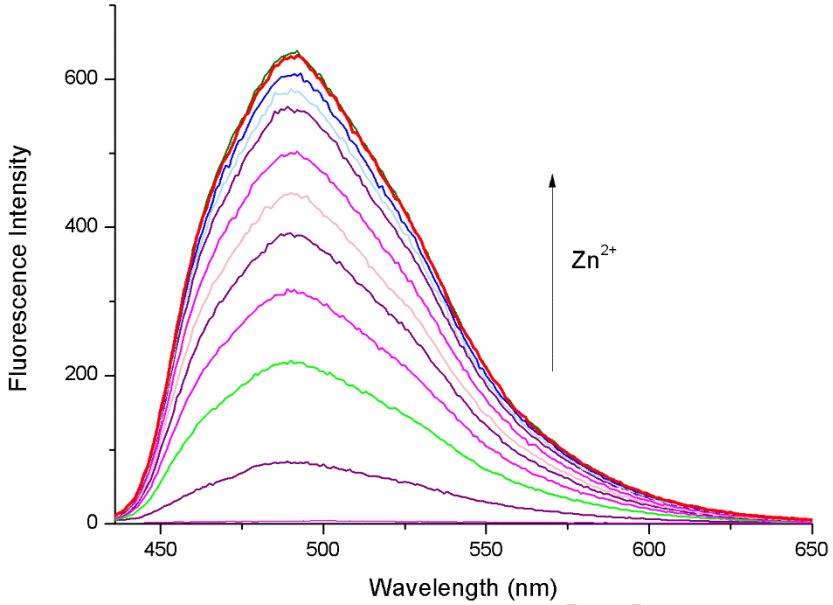

Fig. 4. Fluorescence emission spectra of **L** (50 μM) in EtOH/HEPES solution (3/1, 10.0 μM HEPES, pH 7.4) upon gradual addition of Zn^{2+} (0-1.2 *equiv.*) (λ_{ex} = 421 nm, slit widths: 5 nm/5 nm).

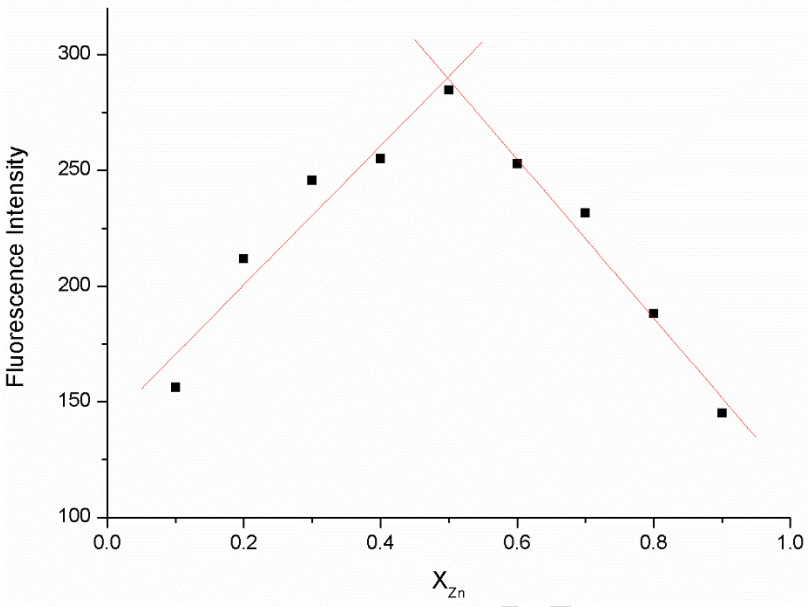

Fig. 5. Job's plot for determining the stoichiometry between probe **L** and Zn^{2+} in EtOH/HEPES solution (3/1, 10.0 μM HEPES, pH 7.4). $X_{Zn} = [Zn^{2+}]/([Zn^{2+}] + [\mathbf{L}])$, the total concentration of **L** and Zn^{2+} was 50 μM (λ_{ex} = 421 nm, slit widths: 5 nm/5 nm).

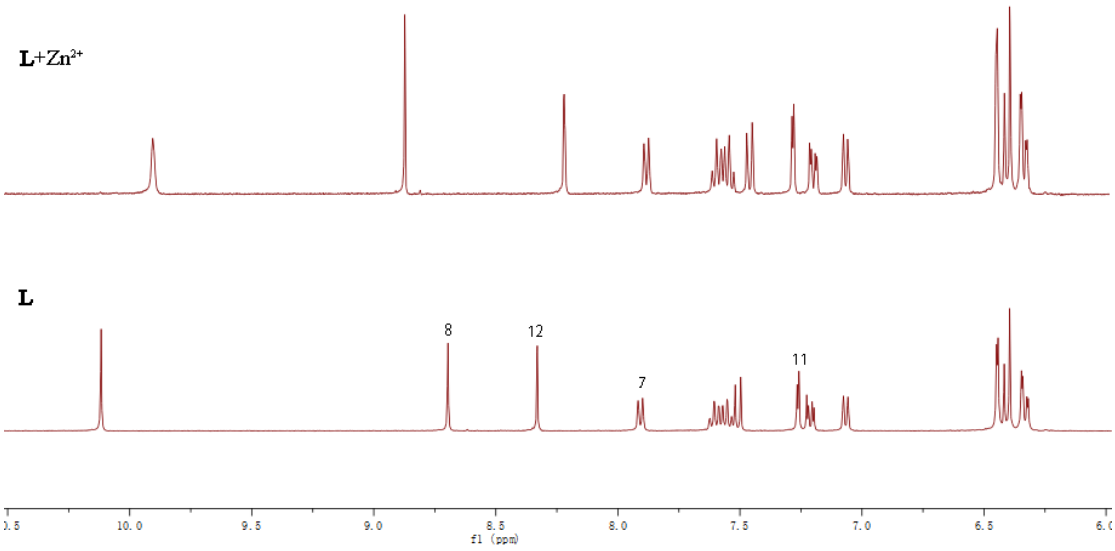

Fig. 6. ^{1}H NMR (DMSO-d_6, 400 MHz) spectra of **L** only and **L** with 1 *equiv.* of Zn^{2+}.

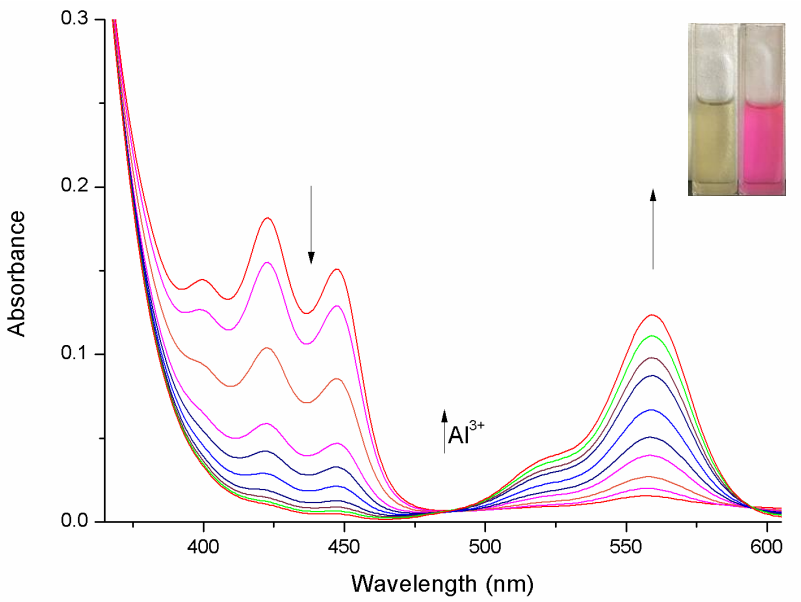

Fig. 7. UV-vis absorption spectra of **LZn** (50.0 μM) in EtOH/MeCN/HEPES solution (6/1/1, 10.0 μM HEPES, pH 7.4) after addition of Al^{3+} (0, 0.1, 0.2, 0.3, 0.4, 0.5, 0.6, 0.7, 0.8, 0.9, 1.0 *equiv.*). Insert: the color changes of **LZn** solution (50.0 μM) in the absence and presence of Al^{3+} (1.0 *equiv.*).

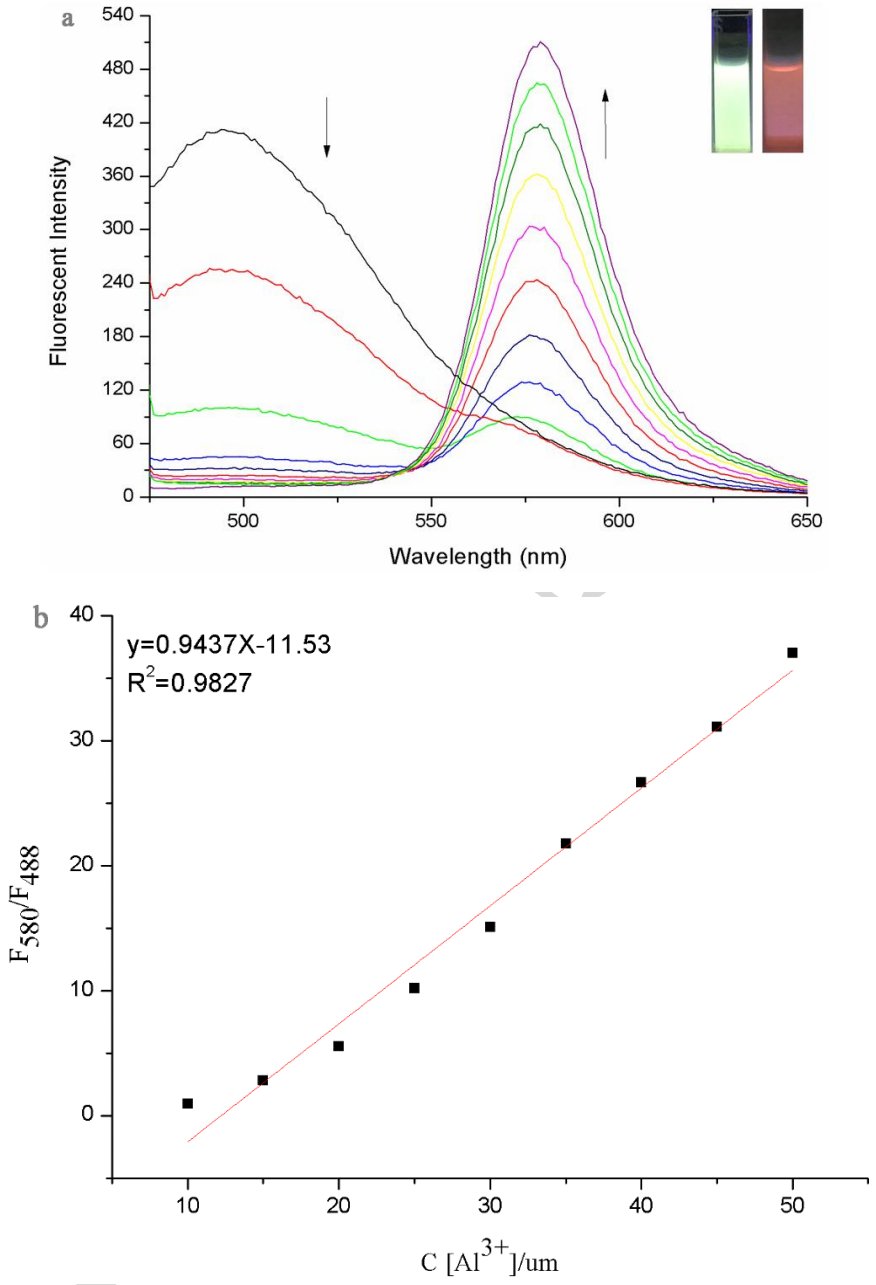

Fig. 8. (a) Fluorescence emission spectra of **LZn** (50 μM) in EtOH/MeCN/HEPES solution (6/1/1, 10.0 μM HEPES, pH 7.4) upon gradual addition of Al^{3+} (0-1.0 *equiv.*) (λ_{ex} = 467 nm, slit widths: 5 nm/5 nm). Inset: color of **LZn** (left) and **LZn** + Al^{3+} (right) system under UV lamp; (b) Plot of relative fluorescence intensity ratio (F_{580}/F_{488}, λ_{ex} = 467 nm) as a function of [Al^{3+}].

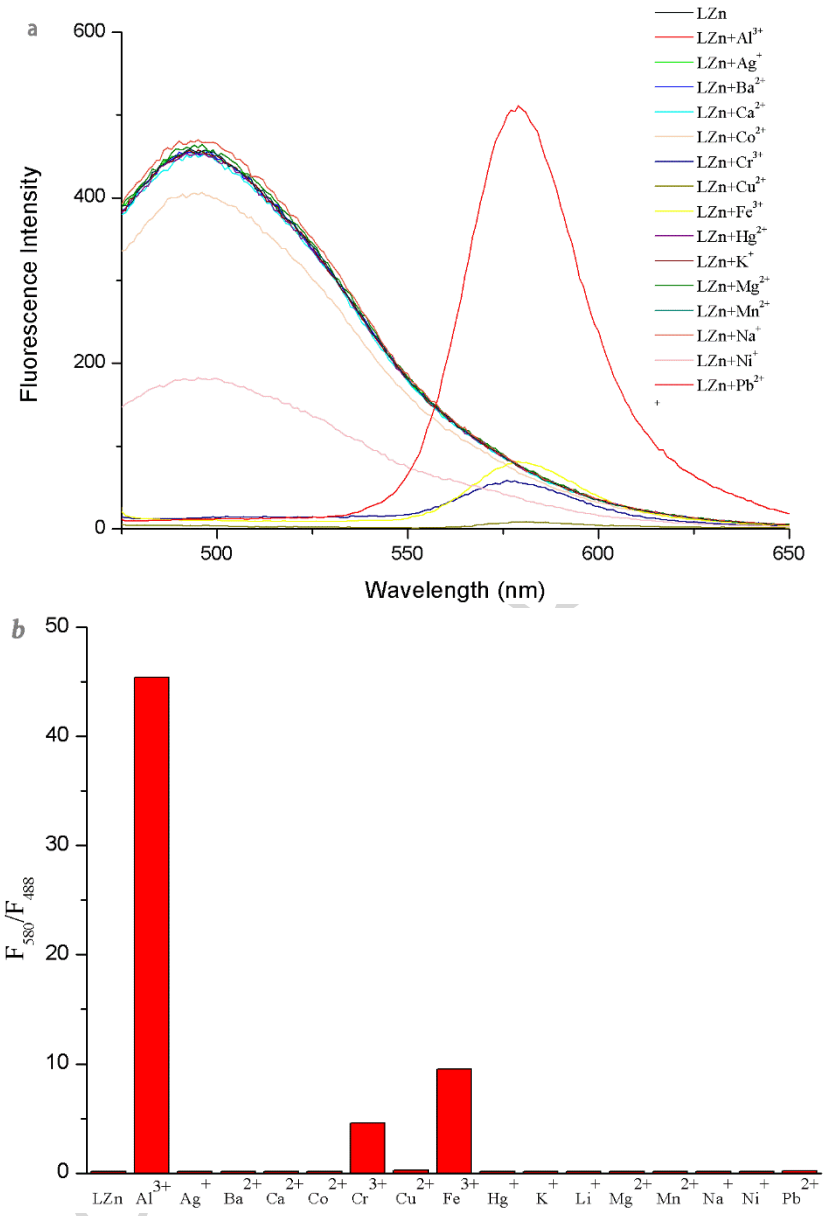

Fig. 9. (a) Fluorescence emission spectra of **LZn** (50 μM) upon the addition of various metal ions (Ag^{+}, Ba^{2+}, Ca^{2+}, Co^{2+}, Cr^{3+}, Cu^{2+}, Fe^{3+}, Hg^{+}, K^{+}, Li^{+}, Mg^{2+}, Mn^{2+}, Na^{+}, Ni^{+}, Pb^{2+} and Al^{3+}) (1.0 *equiv.*) in EtOH/MeCN/HEPES solution (6/1/1, 10.0 μM HEPES, pH 7.4); (b) Relative fluorescence intensity ratio (F_{580}/F_{488}, λ_{ex} = 467 nm) of **LZn** (50 μM) in the absence and presence of various metal ions in EtOH/MeCN/HEPES solution (6/1/1, 10.0 μM HEPES, pH 7.4) (λ_{ex} = 467 nm, slit widths: 5 nm/5 nm).

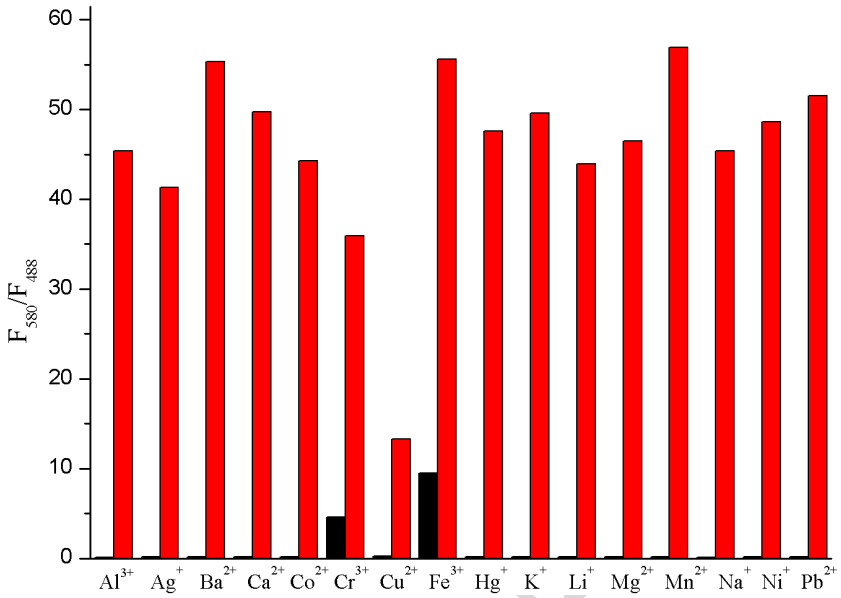

Fig. 10. The ratio of fluorescence emission intensity at 580 nm and 488 nm (F_{580}/F_{488}) of **LZn** and its complexation with Al^{3+} in the presence of other various metal ions (Ag^{+}, Ba^{2+}, Ca^{2+}, Co^{2+}, Cr^{3+}, Cu^{2+}, Fe^{3+}, Hg^{+}, K^{+}, Li^{+}, Mg^{2+}, Mn^{2+}, Na^{+}, Ni^{+} and Pb^{2+}) in EtOH/MeCN/HEPES solution (6/1/1, 10.0 μM HEPES, pH 7.4). Black bar: **LZn** (50.0 μM) in the presence of 1.0 *equiv.* of various metal ions. Red bar: **LZn** (50.0 μM) with 1.0 *equiv.* of Al^{3+} in the presence of 1.0 *equiv.* of other various metal ions (λ_{ex} = 467 nm, slit widths: 5 nm/5 nm).

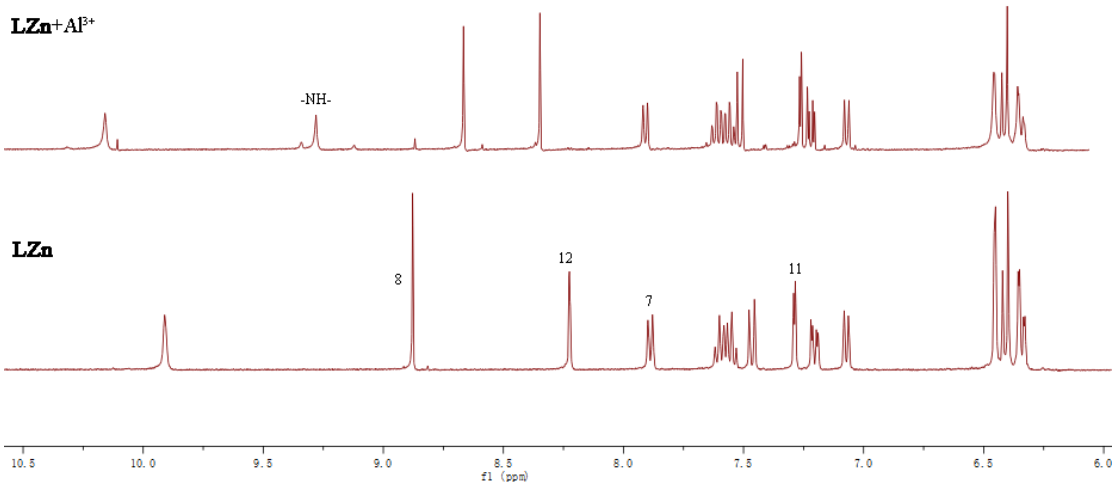

Fig. 11. ^{1}H NMR (DMSO-d_6, 400 MHz) spectra of **L** with 1 *equiv.* of Zn^{2+} (**LZn**); **LZn** with 1 *equiv.* of Al^{3+}.

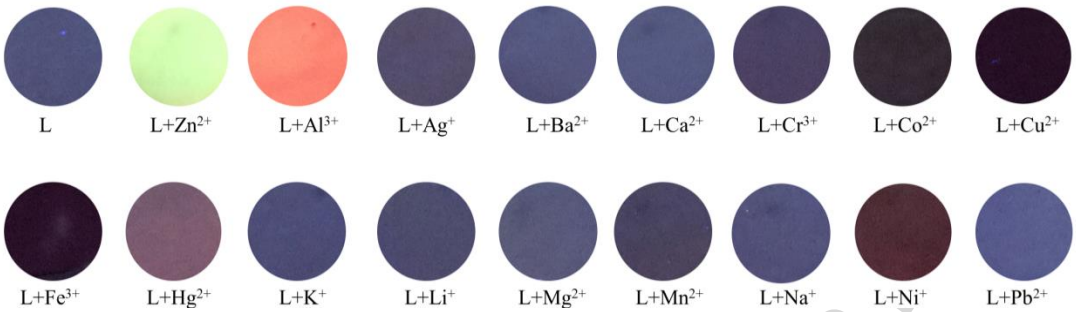

Fig. 12. The photographs of coated test papers after addition of different metal ions under illumination using a 365 nm UV lamp.

Table 1. Comparison of different properties of **L** and **LZn** with recently reported probes based on rhodamine derivatives.

Recognition	**Type**	**ligand-metal complex as a fluorescent probe**	**Reference**
Hg^{2+}	turn on	No	[34]
Hg^{2+}	ratiomrtric	No	[35]
Cu^{2+}	turn on	No	[40]
Hg^{2+}	ratiometric	Yes	[44]
Al^{3+} and Cu^{2+}	turn on/turn on	No	[30]
Pb^{2+} and Al^{3+}	turn on/turn on	No	[32]
Zn^{2+} and Al^{3+}	**turn on/raiometric**	**Yes**	**This study**

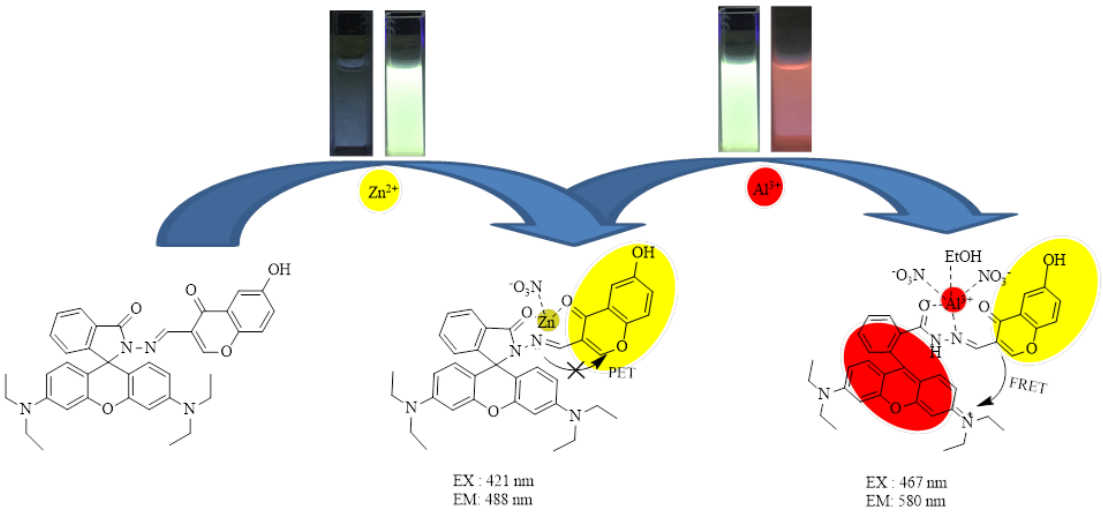

Scheme 2. Proposed binding mechanism of **L** with Zn^{2+} and **LZn** with Al^{3+}.

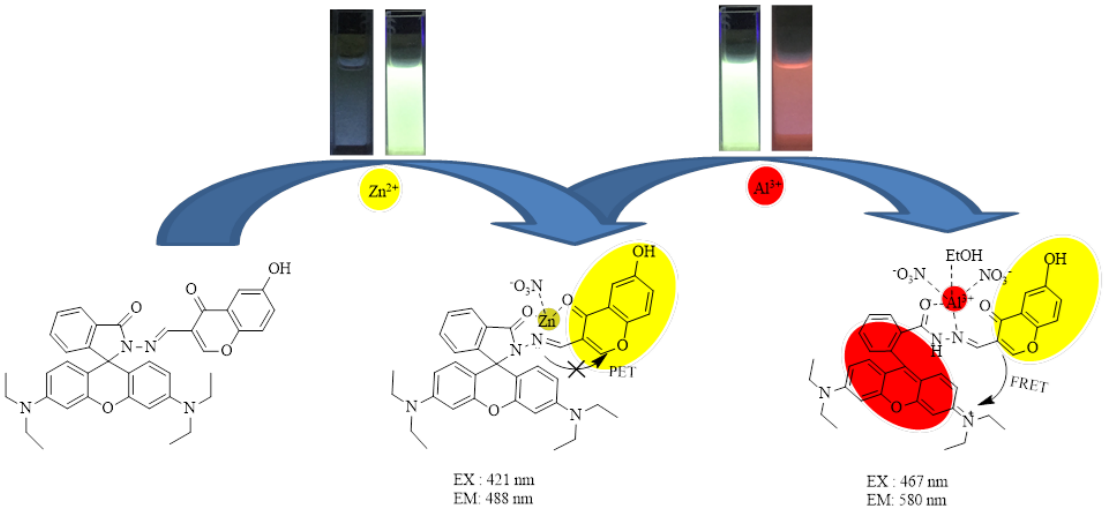

Graphical abstract

Highlights

- A novel fluorescent probe **L** for the detection of Zn(Ⅱ) and Al(Ⅲ) based on two different mechanisms was synthesized.
- The prepared Zn^{2+} complex of **L** (**LZn**) was used as a ratiometric fluorescent probe to detect Al^{3+}.
- Good selectivity of **L** towards Zn^{2+} and **LZn** towards Al^{3+} were observed.
- This probe **L** demonstrated an excellent fluorescence sensing performance even in the solid state.